

## Correlated decays of pair-produced scalar taus

Kaoru Hagiwara<sup>1,2</sup> and Kentarou Mawatari<sup>1y</sup><sup>1</sup>Theory Group, KEK, Tsukuba 305-0801, JAPAN<sup>2</sup>Dept. of Particle and Nuclear Physics, Graduate Univ. for Advanced Studies, Tsukuba 305-0801, JAPANDavid Rainwater<sup>2</sup>

Dept. of Physics and Astronomy, Univ. of Rochester, Rochester, NY 14627, USA

Tim Stelzer<sup>x</sup>

Dept. of Physics, Univ. of Illinois at Urbana-Champaign,

1110 West Green Street, Urbana, Illinois 61801, USA

(Dated: May 24, 2019)

We study the quantum mechanical correlation between two identical neutralinos in the decays of MSSM scalar tau (stau) pair produced in  $e^+ e^-$  annihilation. Generally, the decay products of scalar (spinless) particles are not correlated. We show that a correlation between two neutralinos appears near pair production threshold, due to a finite stau width and mixing of the staus and/or neutralinos, and because the neutralinos are Majorana. Because the correlation is significant only in a specific kinematical configuration, it can be observed only in supersymmetric models where the neutralino momenta can be kinematically reconstructed, such as in models with R-parity violation.

PACS numbers: 14.80.Mz, 13.66.Hk, 12.60.Jv

Keywords: Majorana nature, Correlated decays

## I. INTRODUCTION

Neutralinos are mixtures of the spin-1/2 superpartners of the neutral gauge and Higgs bosons in supersymmetric extensions to the Standard Model. The lightest one ( $\tilde{\chi}_1^0$ ) is generally considered to be the lightest supersymmetric particle (LSP), which is stable in R-parity conserving scenarios. Signals of supersymmetry (SUSY) are expected to be observable at hadron [1] or future  $e^+ e^-$  colliders [2].

In the minimal supersymmetric Standard Model (MSSM), neutralinos are Majorana fermions whose antiparticles are themselves. If SUSY (and the associated neutralinos) is observed in nature, the determination of their properties under CP conjugation, Majorana vs. Dirac, will be a key issue: it is intimately related to the dimension of SUSY, e.g.  $N = 1$  or  $N = 2$  SUSY [3].

Many studies of the Majorana nature of neutralinos have been performed. Ref. [4] observed that the CP and CPT properties of the final-state determine the Majorana nature of neutralinos in the process  $e^+ e^- \rightarrow \tilde{\chi}_1^0 \tilde{\chi}_1^0$ . Selectron pair production in  $e^+ e^-$  scattering,  $e^+ e^- \rightarrow e^+ e^-$ , would also be of great utility, as it could proceed only on account of off-channel Majorana neutralino exchange [5]. In addition, Majorana effects in  $\tilde{\chi}_1^0 \tilde{\chi}_1^0 \rightarrow Z$  decays are known to exist [6].

In this article, we study the Majorana nature of neutralinos in lighter scalar tau (stau) pair production and

subsequent decay into lepton (tau) plus LSP neutralino in  $e^+ e^-$  annihilation,

$$e^+ e^- \rightarrow \tilde{\chi}_1^0 \tilde{\chi}_1^0 \rightarrow \ell \nu \tilde{\chi}_1^0 \tilde{\chi}_1^0; \quad (1)$$

via the quantum mechanical correlation between two identical neutralinos which exists only if they are Majorana fermions. That a correlation should exist should be evident simply due to proper treatment of the Fermi statistics of the final-state neutralinos, but it is always ignored: conventional wisdom says that the correlation between decay products of scalar (spinless) particles, such as staus, is absent. Because of this, little attention in the literature has been given to the expected Majorana effect, even though the process we consider here is among the most promising to study SUSY particles and many studies of it have been performed [7, 8] for exploration of other aspects. Naturally, no correlation is possible once a spinless particle is separated from the other particles at a macroscopic space-time distance. In other words, any interference effect disappears in the limit of long lifetime of the spinless particles. We should hence consider the finite stau width, and investigate the region near pair production threshold.

In addition to the finite width, the left-right mixing of the staus and/or the gaugino-higgsino mixing of the neutralinos are necessary for the correlation to be significant. This is because in the massless neutralino limit, same-helicity neutralinos are produced only when the taus have the same helicity, which occurs only when the  $\tilde{\chi}_L \tilde{\chi}_R$  mixing and/or the neutralino mixing are significant. We will discuss this in detail in the following section, and simply note in passing that significant interference effects are expected in  $e_L e_R$  and  $\tilde{\chi}_L \tilde{\chi}_R$  pair production processes, which quantitative study will be reported elsewhere.

E-mail address: kaoru.hagiwara@kek.jp

yE-mail address: kentarou@post.kek.jp

zE-mail address: rain@pas.rochester.edu

xE-mail address: tstelzer@uiuc.edu

The article is organized as follows. Sec. II gives a brief introduction of the mass eigenstates of the staus ( $\tilde{\chi}_1, \tilde{\chi}_2$ ) and the gaugino-higgsino mixing of the neutralinos. The  $\tilde{\chi}_1 - \tilde{\chi}_1^0$  coupling is also given. In Sec. III, we present scattering amplitudes for the process  $e^+ e^- \rightarrow \tilde{\chi}_1^+ \tilde{\chi}_1^-$  and define the kinematical variables relevant to our analysis. Sec. IV gives the total cross sections around the  $\tilde{\chi}_1$  pair production threshold. In Sec. V, we study in detail the kinematical correlations due to identical-particle interference effects and compare them to the Dirac (non-interference) case. Sec. VI is devoted to a summary and discussions.

## II. STAU AND NEUTRALINO MIXING

In this section, we briefly introduce the staus' left-right mixing and the neutralinos' gaugino-higgsino mixing. We also give the  $\tilde{\chi}_1 - \tilde{\chi}_1^0$  coupling, where  $\tilde{\chi}_1$  is defined to be the lighter stau mass eigenstate after L-R mixing.

Because of the non-negligible tau Yukawa coupling, mixing occurs between the weak eigenstates  $\tilde{\chi}_L$  and  $\tilde{\chi}_R$  to form mass eigenstates  $\tilde{\chi}_1$  and  $\tilde{\chi}_2$  ( $m_{\tilde{\chi}_1} < m_{\tilde{\chi}_2}$ ) as

$$\begin{aligned} \tilde{\chi}_L &= \cos \tilde{\alpha} \tilde{\chi}_L + \sin \tilde{\alpha} \tilde{\chi}_R \\ \tilde{\chi}_R &= -\sin \tilde{\alpha} \tilde{\chi}_L + \cos \tilde{\alpha} \tilde{\chi}_R \end{aligned} \quad (2)$$

Neutralinos are mass eigenstates of the neutral gauginos,  $B^0$  and  $W_3^0$ , and the neutral higgsinos,  $H_d^0$  and  $H_u^0$ . The mass matrix in the  $X = (B^0; W_3^0; H_d^0; H_u^0)$  basis is

$$M = \begin{pmatrix} 0 & M_1 & 0 & m_z s_w c & m_z s_w s & 1 \\ B^0 & 0 & M_2 & m_z c_w c & m_z c_w s & 0 \\ m_z s_w c & m_z c_w c & 0 & & & A \\ m_z s_w s & m_z c_w s & & & & 0 \end{pmatrix} \quad (3)$$

with the abbreviations  $s_w = \sin w$ ,  $c_w = \cos w$ ,  $s = \sin \theta$ , and  $c = \cos \theta$ . Here,  $M_1$  and  $M_2$  are the gaugino masses,  $\tilde{\alpha}$  is the higgsino mass, and  $\tan \theta = h_u^0/h_d^0$  is the ratio of the vacuum expectation values of the two Higgs doublets. The mass eigenstates are given by

$$X_1 = U_{ij} \tilde{\chi}_j^0; \quad (4)$$

where  $U$  diagonalizes the above mass matrix as

$$U^T M U = \text{diag}(m_{\tilde{\chi}_1^0}; m_{\tilde{\chi}_2^0}; m_{\tilde{\chi}_3^0}; m_{\tilde{\chi}_4^0}); \quad (5)$$

Here,  $0 < m_{\tilde{\chi}_1^0} < m_{\tilde{\chi}_2^0} < m_{\tilde{\chi}_3^0} < m_{\tilde{\chi}_4^0}$ .

The decay  $\tilde{\chi}_1^0 \rightarrow \tilde{\chi}_1 \tilde{\chi}_1$  depends on both the left-right stau mixing ( $\tilde{\alpha}$ ) and the neutralino mixing ( $U_{ij}$ ). The  $\tilde{\chi}_1 - \tilde{\chi}_1^0$  coupling can be expressed as

$$L = \overline{\tilde{\chi}_1^0} (a_- P_- + a_+ P_+) \tilde{\chi}_1 + \text{h.c.}; \quad (6)$$

with the chiral projection operators  $P_\pm = \frac{1}{2}(1 \pm \gamma_5)$ . We denote left-handed (L) by  $_-$  and right-handed (R) by  $+$  for notational convenience. The complex couplings  $a$  are expressed in terms of the  $\tilde{\chi}_L - \tilde{\chi}_L^0$  and  $\tilde{\chi}_R - \tilde{\chi}_R^0$  couplings,  $a^L$  and  $a^R$ , respectively, as

$$a = \cos \tilde{\alpha} \tilde{a} + \sin \tilde{\alpha} \tilde{b}; \quad (7)$$

Here,

$$\begin{aligned} a^L &= \frac{g}{2} (U_{21} + U_{11} \tan w); & a^R &= U_{31} Y; \\ a_+^R &= -\frac{g}{2} 2 U_{11} \tan w; & a_+^L &= U_{31} Y; \end{aligned} \quad (8)$$

where  $Y = g m = (\frac{g}{2} m_w \cos \theta)$  and  $g$  is the  $SU(2)_L$  gauge coupling. The couplings  $a^L$  and  $a_+^R$  come from the stau-gaugino interactions, where chirality is conserved. On the other hand,  $a^R$  and  $a_+^L$  are proportional to the tau mass, and come from the  $\tilde{\chi}_1 - H_d^0$  Yukawa coupling, which breaks chirality. For further details see Ref. [8].

At this point it is worth noting that either the left-right stau mixing or the gaugino-higgsino mixing of the neutralinos is needed for the Majorana interference effects to be significant. This may be explained as follows: if both mixings are absent, the tau produced in decay is either left-handed (gaugino interaction) or right-handed (higgsino interaction), and the  $\tilde{\chi}_1$  is of the opposite chirality. The two neutralinos then have opposite chirality and their interference vanishes in the massless limit, where helicity coincides with chirality.

## III. AMPLITUDES AND KINEMATICS

In this section we present helicity amplitude formulae for the process

$$\begin{aligned} e^-(k_1; \tilde{\alpha}) + e^+(k_2; \tilde{\alpha}) &\rightarrow \tilde{\chi}_1^+ + \tilde{\chi}_1^- \\ &\rightarrow (k_1; \tilde{\chi}_1^0) + \tau^+ (k_2; \tilde{\chi}_1^0) + \tilde{\chi}_1^0(p_1; \tilde{\chi}_1^0) + \tilde{\chi}_1^0(p_2; \tilde{\chi}_1^0); \end{aligned} \quad (9)$$

where the four-momentum and helicity of each particle are defined in the center-of-mass (CM) frame of the  $e^+ e^-$  collision. If neutralinos are Majorana fermions, the two neutralinos ( $\tilde{\chi}_1^0$ ) in the final state are identical. Therefore the crossed diagram (b) of Fig. 1 should be added to diagram (a) before the amplitude is squared. The relative sign between these two diagrams appears due to Fermi statistics.

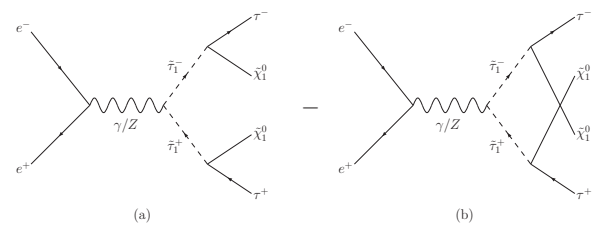


FIG. 1: Feynman diagrams for the process  $e^+ e^- \rightarrow \tilde{\chi}_1^0 \tilde{\chi}_1^0$ .

The full amplitude can be expressed as the product of the stau pair production amplitude ( $M_{\sim}$ ), the two Breit-Wigner propagators for the staus,

$$D_{\sim}(q^2) = (q_1^2 - m_{\tilde{\chi}_1}^2 + i m_{\tilde{\chi}_1} \gamma_1)^{-1}; \quad (10)$$

and two  $\tilde{\chi}_1$  !  $\tilde{\chi}_1^0$  decay amplitudes ( $M_{\sim}$  and  $\overline{M}_{\sim}$ ). That is,

$$\begin{aligned} M_{\sim} &= M_{\sim}(\tilde{\chi}_1; \tilde{\chi}_2; \tilde{\chi}_1; \tilde{\chi}_2) \\ &= M_{\sim}(\tilde{\chi}_1; q_1^0; q_2^0) D_{\sim}(q_1^2) D_{\sim}(q_2^2) M_{\sim}(q_1; \tilde{\chi}_1; \tilde{\chi}_1) \overline{M}_{\sim}(q_2; \tilde{\chi}_2; \tilde{\chi}_2) \\ &= M_{\sim}(\tilde{\chi}_1; q_1^0; q_2^0) D_{\sim}(q_1^0)^2 D_{\sim}(q_2^0)^2 M_{\sim}(q_1^0; \tilde{\chi}_1; \tilde{\chi}_2) \overline{M}_{\sim}(q_2^0; \tilde{\chi}_2; \tilde{\chi}_1) \\ &= M_{\tilde{\chi}_1} M_{\tilde{\chi}_2}; \end{aligned} \quad (11)$$

The intermediate stau momenta can be written in terms of the final state particle momenta:  $q_1 = k_1 + p_1$ ,  $q_2 = k_2 + p_2$ ,  $q_1^0 = k_1 + p_2$ , and  $q_2^0 = k_2 + p_1$ . The stau pair production amplitude is given by

$$M_{\sim}(\tilde{\chi}_1; q) = \frac{e^2 h}{s} \frac{1}{1 + \frac{s}{s - m_Z^2 + i m_Z \gamma_Z}} g_{-} (g_{-} \cos^2 \gamma_{\sim} + g_{+} \sin^2 \gamma_{\sim}) \bar{u}(k_1; \gamma_{\sim}) u(k_1; \gamma_{\sim}); \quad (12)$$

with Z boson couplings to left- and right-handed charged leptons,  $g_{-} = \frac{1+2s_W^2}{2s_W c_W}$  and  $g_{+} = \frac{s_W}{c_W}$ , respectively. Here, we neglect the electron mass and take  $\gamma_{\sim} = \pi/2$ . Using the straightforward Feynman rules for Majorana fermions given in Ref. [9], the stau decay amplitudes for  $M_{\tilde{\chi}_1}$  are written as

$$\begin{aligned} M_{\sim}(q_1; \tilde{\chi}_1; \tilde{\chi}_1) &= \bar{u}(k_1; \tilde{\chi}_1) (a_{-} P_{+} + a_{+} P_{-}) v(p_1; \tilde{\chi}_1); \\ \overline{M}_{\sim}(q_2; \tilde{\chi}_2; \tilde{\chi}_2) &= \bar{u}(p_2; \tilde{\chi}_2) (a_{-} P_{+} + a_{+} P_{-}) v(k_2; \tilde{\chi}_2); \end{aligned} \quad (13)$$

Similarly, for  $M_{\tilde{\chi}_2}$

$$\begin{aligned} M_{\sim}(q_1^0; \tilde{\chi}_1; \tilde{\chi}_2) &= \bar{u}(k_1; \tilde{\chi}_1) (a_{-} P_{+} + a_{+} P_{-}) v(p_2; \tilde{\chi}_2); \\ \overline{M}_{\sim}(q_2^0; \tilde{\chi}_2; \tilde{\chi}_1) &= \bar{u}(p_1; \tilde{\chi}_1) (a_{-} P_{+} + a_{+} P_{-}) v(k_2; \tilde{\chi}_2); \end{aligned} \quad (14)$$

In this article, we assume the lighter stau ( $\tilde{\chi}_1$ ) to be the next-to-lightest supersymmetric particle (NLSP), a common occurrence in many MSSM scenarios. Hence, all  $\tilde{\chi}_1$ 's decay into  $\tilde{\chi}_1^0$  plus  $\tilde{\chi}_1^0$ , and the total decay width  $\tilde{\chi}_1$  is just the partial width ( $\tilde{\chi}_1$  !  $\tilde{\chi}_1^0$ ). Using the  $\tilde{\chi}_1$  decay amplitude  $M_{\sim}$  in Eq. (13), the decay width is given by

$$\tilde{\chi}_1 = (\tilde{\chi}_1 ! \tilde{\chi}_1^0) = \frac{1}{2m_{\tilde{\chi}_1}} \int_{\tilde{\chi}_1; \tilde{\chi}_1}^Z X \overline{M}_{\sim}(q_1; \tilde{\chi}_1; \tilde{\chi}_1) \bar{f} d_{\tilde{\chi}_2} = \frac{1}{16} \bar{p}_{\tilde{\chi}_1} \bar{f} + \bar{p}_{\tilde{\chi}_1} \bar{f} m_{\tilde{\chi}_1} \frac{1}{1 - \frac{m_{\tilde{\chi}_1}^2}{m_{\tilde{\chi}_1}^2}}; \quad (15)$$

with  $m_{\tilde{\chi}_1} = 0$  and the Lorentz-invariant phase space factor

$$d_{\tilde{\chi}_1} p = \prod_{i=1}^{X^n} k_i = (2\pi)^{4-n} p \prod_{i=1}^{X^n} k_i \prod_{i=1}^{Y^n} \frac{d^3 k_i}{(2\pi)^3 2k_i^0}; \quad (16)$$

Throughout our study we neglect the tau mass, except in  $Y$  of the  $\tilde{\chi}_1$  !  $\tilde{\chi}_1^0$  coupling, given in Eq. (8).

Let us now define the kinematical variables. In the CM frame of the  $e^+ e^-$  annihilation, we choose the  $\tilde{\chi}_1$  momentum direction as the z-axis,

$$\begin{aligned} q_1 &= \frac{p \bar{s}}{2} \left( 1 + \frac{q_1^2 - q_2^2}{s} \right); 0; 0; \quad ; \\ q_2 &= \frac{p \bar{s}}{2} \left( 1 + \frac{q_2^2 - q_1^2}{s} \right); 0; 0; \quad ; \end{aligned} \quad (17)$$

where  $\bar{s} = (\frac{q_1^2}{s}; \frac{q_2^2}{s})$  with  $(a; b) = (1 + a^2 + b^2 - 2a - 2b - 2ab)^{1/2}$ , and we choose the  $\tilde{\chi}_1$   $q_1$  direction as the y-axis. For computational convenience, we parametrize the momenta of  $\tilde{\chi}_1$  and  $\tilde{\chi}_1^0$  with  $p_1$  in the rest frame of  $q_1$ ,

$$\begin{aligned} k_1 &= \frac{p \bar{q}_1^2}{2} \left( 1 - \frac{m_{\tilde{\chi}_1}^2}{q_1^2} \right); \tilde{\chi}_1 \sin \tilde{\chi}_1 \cos \tilde{\chi}_1; \tilde{\chi}_1 \sin \tilde{\chi}_1 \sin \tilde{\chi}_1; \tilde{\chi}_1 \cos \tilde{\chi}_1; \\ p_1 &= \frac{p \bar{q}_1^2}{2} \left( 1 + \frac{m_{\tilde{\chi}_1}^2}{q_1^2} \right); \tilde{\chi}_1 \sin \tilde{\chi}_1 \cos \tilde{\chi}_1; \tilde{\chi}_1 \sin \tilde{\chi}_1 \sin \tilde{\chi}_1; \tilde{\chi}_1 \cos \tilde{\chi}_1; \end{aligned} \quad (18)$$

with  $\gamma_1 = 1$  and  $m_{\tilde{\chi}_1^0}^2 = q_1^2$ . Those of  $\tau^+$  and  $\tilde{\chi}_1^0$  with  $p_2$  are then in the  $q_2$  rest frame,

$$\begin{aligned} k_2 &= \frac{p}{\frac{q_2^2}{2}} \left( 1 - \frac{m_{\tilde{\chi}_1^0}^2}{q_2^2} \right) \tau_2^+ \sin_2 \cos_2; \tau_2^+ \sin_2 \sin_2 \tau_2^+ \cos_2; \\ p_2 &= \frac{p}{\frac{q_2^2}{2}} \left( 1 + \frac{m_{\tilde{\chi}_1^0}^2}{q_2^2} \right) \tau_2^+ \sin_2 \cos_2; \tau_2^+ \sin_2 \sin_2 \tau_2^+ \cos_2; \end{aligned} \quad (19)$$

with  $\gamma_2 = 1$  and  $m_{\tilde{\chi}_1^0}^2 = q_2^2$ . The two frames differ only by a boost along the  $z$ -axis (see Fig. 2). All the frame-dependent variables with a star superscript ( $*$ ) are those in the  $\gamma_1$  rest frame.

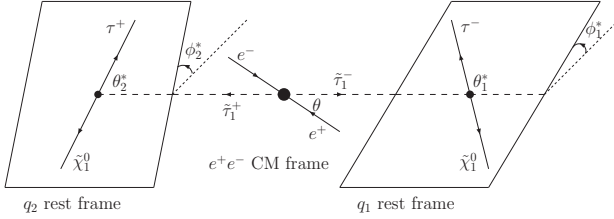


FIG. 2: Schematic view of the coordinate system.

Before turning to the numerical study, it is worthwhile to mention the relation of the helicities between the taus ( $\tau_{1,2}$ ) and the neutralinos ( $\tilde{\chi}_{1,2}$ ). Generally, when a scalar (spinless) particle decays into two fermions, they always have the same helicity in the rest frame of the parent, due to helicity conservation in gauge interactions. In the massless neutralino limit, this relation remains even in the  $e^+e^-$  CM frame since the spin cannot flip due to the boost, i.e.,

$$\begin{aligned} \tau_1 &= \tilde{\chi}_1^0 \text{ and } \tau_2 = \tilde{\chi}_2^0 \text{ for } M_1; \\ \tau_1 &= \tilde{\chi}_2^0 \text{ and } \tau_2 = \tilde{\chi}_1^0 \text{ for } M_2; \end{aligned} \quad (20)$$

Therefore, in the massless neutralino and tau limit, when  $\tau^+$  and  $\tau^-$  have the same helicity ( $\tau_1 = \tau_2$ ), the two neutralinos also have the same helicity, and we expect significant interference effects between the two amplitudes,  $M_1$  and  $M_2$ . On the other hand, there is no interference for the  $\tau_1 \neq \tau_2$  case since either the amplitude  $M_1$  or  $M_2$  vanishes. For finite neutralino mass, however, the simple relations between the helicities in Eq. (20) do not hold due to the spin-flip effects due to Lorentz boosts. Interference effects can then appear even for the  $\tau_1 \neq \tau_2$  case. In the following, we always sum over neutralino helicities, but not tau helicities. Notice that the tau polarizations are observable statistically from their decay distributions.

In order to confirm the above kinematical analysis, we consider the interference term analytically. In the spin-summed squared amplitude  $M^2 = M_1^2 + M_2^2$  (cf. Eq. (11)), the interference term is given by the real part of  $M_1 M_2$  as

$$I = \frac{1}{2} \operatorname{Re} \sum_{\tau_1, \tau_2} M_1 M_2; \quad (21)$$

where we sum over the initial electron polarizations ( $\tau$ ) and the neutralino polarizations ( $\tilde{\chi}_1$  and  $\tilde{\chi}_2$ ), but keep the helicities ( $\tau_1$  and  $\tau_2$ ) fixed. The minus sign is the result of Fermi statistics. The interference term  $I$  can be expressed as the product of the production part  $I_P$ , the Breit-Wigner propagator part, and the decay part  $I_D$ :

$$I = 2 \operatorname{Re} I_P \sum_{\tau} (q_1^2) D \sim (q_2^2) D \sim (q_1^0)^2 D \sim (q_2^0)^2; \quad (22)$$

where

$$I_P = \sum_{\tau} M \sim ( ; q_1^0; q_2^0) M \sim ( ; q_1^0; q_2^0); \quad (23)$$

$$\begin{aligned} I_D = & \sum_{\tau_1, \tau_2} M \sim (q_1^0; \tau_1; \tau_1) \overline{M} \sim (q_2^0; \tau_2; \tau_2) \\ & M \sim (q_1^0; \tau_1; \tau_2) \overline{M} \sim (q_2^0; \tau_2; \tau_1); \end{aligned} \quad (24)$$

Note that we include the minus sign explicitly in the production part. For the decay part, using the  $\gamma_1$  decay amplitudes of Eqs. (13) and (14), the relations

$$\begin{aligned} & \sum_{\tau} u^T(p; s) v(p; s) = C^{-1} \not{p} \not{m}; \\ & v(p; s) u^T(p; s) = \not{p} \not{m} C^T; \end{aligned} \quad (25)$$

and the properties of the charge conjugation matrix  $C$ , we obtain

$$I_D = \begin{cases} \not{p}_1 \not{p}_2 \operatorname{tr} \not{E}_1 \not{E}_1 \not{E}_2 \not{E}_2 & \text{for } \tau_1 = \tau_2; \\ \frac{1}{2} m_{\tilde{\chi}_1^0}^2 \not{p}_1^4 + \not{p}_2^4 \operatorname{tr} \not{E}_1 \not{E}_2 & \text{for } \tau_1 \neq \tau_2; \end{cases} \quad (26)$$

This confirms the above kinematical analysis.

#### IV. TOTAL CROSS SECTIONS

In this section, we present total cross section for the process  $e^+e^- \rightarrow \tau^+ \tilde{\chi}_1^0 \tilde{\chi}_1^0$  around and well below the  $\gamma_1$  pair production threshold. In addition to the double-resonance contribution (Fig. 1) which we have discussed so far, we further consider the single-resonance contributions to the final states, shown in Fig. 3. There are two additional diagrams, each having its own crossed diagram for the Majorana neutralino case.

The cross section for the process  $e^+e^- \rightarrow \tau^+ \tilde{\chi}_1^0 \tilde{\chi}_1^0$  averaged over initial electron polarization and summed

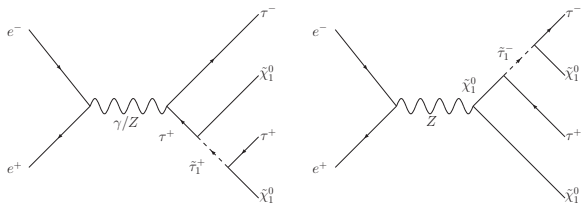


FIG. 3: The single-resonance contributions to the final state  $+\tilde{\chi}_1^0\tilde{\chi}_1^0$  in  $e^+e^-$  annihilation.

over neutralino polarizations reads

$$d_{1-2} = \frac{1}{2s} \frac{1}{4} \sum_{i_1, i_2} M(i_1, i_2; 1, 2) \frac{1}{2} d_4; \quad (27)$$

where  $i_1$  and  $i_2$  are the helicities of  $\tilde{\chi}_1^0$  and  $\tilde{\chi}_2^0$ . In addition to the initial-state spin-average factor, we divide by the statistical factor for two identical neutralinos in the final state. The amplitude  $M$  is summed over all diagrams; not only the double-resonance contributions in Eq. (11), but also the single-resonance contributions. The four-body phase space factor  $d_4$  can be decomposed as the two-body phase space  $d_2$ , and can be parametrized by the kinematical variables defined in Eqs. (17)–(19) as

$$\begin{aligned} d_4 &= d_2(k + k = q_1 + q_2) \frac{dq_1^2}{2} \frac{dq_2^2}{2} \\ &\quad d_2(q_1 = k_1 + p_1) d_2(q_2 = k_2 + p_2) \\ &= \frac{1}{2} \frac{2}{(32^2)^3} dq_1^2 dq_2^2 d \cos \theta \cos \theta_1 d \cos \theta_2 d \cos \theta_3; \end{aligned} \quad (28)$$

where  $\theta$  is the scattering angle between the  $e^-$  momentum ( $k$ ) and  $q_1$  in the  $e^+e^-$  CM frame (see Fig. 2).

Now let us explain several parameters we use in our numerical analysis. All the helicity amplitudes, including the single-resonance contributions, are calculated by HELAS subroutines [10], and numerical integrations are done with the help of the Monte Carlo integration package BASES [11]. We fix the  $\tilde{\chi}_1^0$  mass at  $m_{\tilde{\chi}_1^0} = 150$  GeV. As for the SUSY parameters, including the left-right stau mixing, we take the following values so that the Majorana effects are expected to be large:

$$\tilde{\chi}_1^0 = 45^\circ; \tan \theta = 50; M_2 = 300 \text{ GeV}; \tilde{\chi}_2^0 = 70 \text{ GeV}; \quad (29)$$

and adopting the mass relation  $M_1 = \frac{5}{3} \tan^2 \theta M_2$ . This parameter set corresponds to a Higgsino-like neutralino LSP. For these parameters, the  $\tilde{\chi}_1^0$  mass is  $m_{\tilde{\chi}_1^0} = 50$  GeV, which yields a  $\tilde{\chi}_1^0$  total decay width of  $\Gamma_{\tilde{\chi}_1^0} = 0.52$  GeV, using Eq. (15).

Fig. 4 shows the helicity-dependent total cross section, Eq. (27), for the process  $e^+e^- \rightarrow +\tilde{\chi}_1^0\tilde{\chi}_1^0$  as a

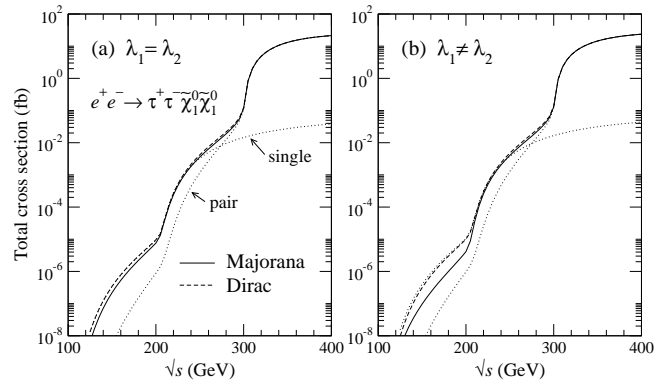


FIG. 4: Total cross section as a function of collision energy, of the process  $e^+e^- \rightarrow +\tilde{\chi}_1^0\tilde{\chi}_1^0$ , for (a)  $\lambda_1 = \lambda_2$  and (b)  $\lambda_1 \neq \lambda_2$ , where  $i_1, i_2$  is the helicity of the  $i$ . Solid and dashed lines show the case that neutralinos are Majorana and Dirac fermions, respectively. Dotted lines are for each contribution from the  $\tilde{\chi}_1^0$  pair and singly-resonant  $\tilde{\chi}_1^0$  production without the interference term.

function of the CM energy  $\sqrt{s}$  in  $e^+e^-$  collisions. In order to show the single-resonance contributions, the cross section is shown starting from rather low values. Solid lines denote the cross sections including the crossed diagrams, such as Fig. 1 (b), which should be present for Majorana neutralinos. The dashed lines are obtained by neglecting the crossed diagrams, which corresponds to Dirac neutralinos. As a reference, each contribution from the  $\tilde{\chi}_1^0$  pair and the single- $\tilde{\chi}_1^0$  production (without the interference term) is shown by dotted lines.

Above the  $\tilde{\chi}_1^0$  pair production threshold ( $\sqrt{s} > 2m_{\tilde{\chi}_1^0} = 300$  GeV) the contribution from  $\tilde{\chi}_1^0$  pair production (Fig. 1) is dominant. Below pair threshold the single-resonance processes (Fig. 3) contribute dominantly, even though the cross section becomes very small. The reduction of the cross section by the interference effects for Majorana neutralinos can be seen below the  $\tilde{\chi}_1^0$  pair and the single- $\tilde{\chi}_1^0$  production thresholds. Unfortunately, the total cross section in the region below threshold where Majorana interference effects become important is not at a level which could be observed.

## V. MAJORANA EFFECTS

We have seen that it is difficult to observe a Majorana interference effect in the total cross section. In this section, we therefore study in detail the kinematical correlations due to interference effects that appear only for Majorana neutralinos. We present several distributions for the process  $e^+e^- \rightarrow +\tilde{\chi}_1^0\tilde{\chi}_1^0$  near the stau pair production threshold, and discuss the Majorana effects as a function of the finite  $\tilde{\chi}_1^0$  width. We consider the following three distributions to see the interference:

- (a)  $\cos \theta_1$ : defined in the  $q_1$  rest frame in Eq. (18) (See Fig. 2);

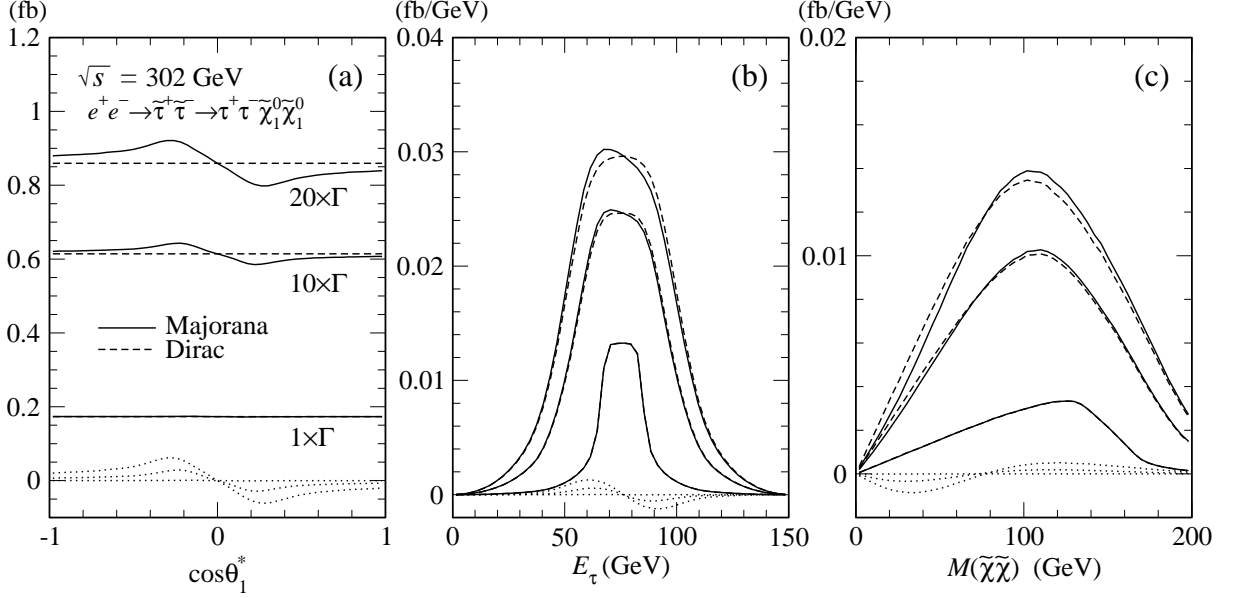


FIG. 5: Distributions of (a)  $\cos \theta_1^*$ , (b)  $E_\tau$ , and (c)  $M(\tilde{\chi}\tilde{\chi})$  for the process  $e^+ e^- \rightarrow \tilde{\tau}^+ \tilde{\tau}^- \rightarrow \tau^+ \tau^- \tilde{\chi}_1^0 \tilde{\chi}_1^0$  at  $\sqrt{s} = 302$  GeV for  $1;10;20$  in the massless neutralino limit. Solid and dashed lines show the Majorana and Dirac neutralino cases, respectively. Also shown is the behavior of the interference term by dotted lines.

(b)  $E_\tau$ : the energy in the laboratory frame;  
 (c)  $M(\tilde{\chi}\tilde{\chi})$ : the invariant mass of the neutralino pair,  
 $M^2 = (p_1 + p_2)^2 = (k + k_1 - k_2)^2$ .

Note that, from the experimental point of view, these variables are not observables, since taus always decay into at least one neutrino, which escapes detection together with the neutralinos; the kinematical system is unconstrained by observables and cannot be reconstructed. Therefore, our studies may be regarded as pedagogical, or may apply to models where the neutralino momenta can be kinematically reconstructed, such as those with R-parity violation.

To begin with, for simplicity we consider only the  $\tilde{\chi}_1$  pair production process  $e^+ e^- \rightarrow \tilde{\tau}^+ \tilde{\tau}^- \rightarrow \tau^+ \tau^- \tilde{\chi}_1^0 \tilde{\chi}_1^0$ , and take the massless neutralino limit.

Fig. 5 shows the distributions of (a)  $\cos \theta_1^*$ , (b)  $E_\tau$ , and (c)  $M(\tilde{\chi}\tilde{\chi})$ , at  $\sqrt{s} = 302$  GeV for the  $\tilde{\chi}_1 = \tilde{\chi}_2$  case. We use the same SUSY parameter set in Eq. (29) as the total cross sections. To examine the finite  $\tilde{\chi}_1$  width effect, we vary the total width  $\tilde{\chi}_1$  as  $1;10;20$ . In the limit of  $\tilde{\chi}_1 = 0$ , the  $\tilde{\chi}_1$  total decay width is

$\tilde{\chi}_1 = 0.66$  GeV from Eq. (15), hence  $10 \tilde{\chi}_1 = 6.6$  GeV and  $20 \tilde{\chi}_1 = 13$  GeV. Above threshold, the wider the decay width, the larger the cross section. Solid and dashed lines show the Majorana and Dirac neutralino cases, respectively. Also shown as a reference is the behavior of the interference term only, Eq. (21), by dotted lines. For the realistic  $\tilde{\chi}_1$  case, the interference patterns are barely discernible in Fig. 5. The contribution of the interference term to the cross section is at most about 0.1%, 3% and 6% for  $1;10$  and  $20 \tilde{\chi}_1$ , respectively. The interference effect is roughly proportional to

the  $\tilde{\chi}_1$  decay width. The following features are worth noting: (i) For the  $\tilde{\chi}_1 \neq \tilde{\chi}_2$  case, there is no interference, as expected from the discussion of Sec. III. (ii) For the Dirac neutralino case, the cross section does not depend on  $\cos \theta_1^*$  or  $\cos \theta_2^*$  since the two produced taus decay independently. On the other hand, for the Majorana case, the distribution is no longer flat. The  $\cos \theta_2^*$  distribution is the same as that of  $\cos \theta_1^*$ , but for a relative sign, according to CP-invariance. (iii) A major portion of the interference pattern disappears when we integrate out the kinematical variables, such as  $\cos \theta_1^*$ ,  $E_\tau$ , or  $M(\tilde{\chi}\tilde{\chi})$ . This is why one can hardly view the correlation effect in the total cross section above pair production threshold in Fig. 4. (iv) As for the  $\tilde{\chi}_1$  dependence of the interference effect, it exists even at higher energies. However, the cross section also grows, and the relative effect of the interference term becomes smaller. Therefore the Majorana effect can be seen only near threshold, even though the cross section is small due to the p-wave threshold factor of  $\tilde{\chi}_1^3$ .

Now we attempt to explain why the interference behaves like a sine curve in Fig. 5. We take two different approaches. One is to consider the interference term, Eq. (21), analytically. Another is, more physically, to investigate them kinematically.

First, let us consider the  $\tilde{\chi}_1$  pair production part of the interference term, Eq. (23), analytically. Using the  $\tilde{\chi}_1$

pair production amplitude of Eq. (12),

$$\begin{aligned} I_p &= \frac{e^4 X}{s^2} \left[ \bar{u}(k; \gamma_1^0 \gamma_2^0) u(k; \gamma_1^0) \bar{u}(k; \gamma_1^0 \gamma_2^0) v(k; \gamma_2^0) \right. \\ &\quad \left. - \frac{4e^4}{s^2} \left[ \bar{u}(k; \gamma_1^0 \gamma_2^0) \bar{u}(k; \gamma_1^0 \gamma_2^0) \right] \right] : \quad (30) \end{aligned}$$

The trace part is given by the dot-products of the kinematical variables in Eqs. (17)–(19). The dependence on the scattering angle  $\theta$  appears only in this part. We integrate it out and obtain

$$\begin{aligned} Z_1 &= \frac{1}{1} \frac{d \cos \theta_1^*}{d \cos \theta_2^*} \\ &= \frac{4e^4}{3} \left[ \frac{h}{2} + \left(1 - \frac{m^2}{q_1^2}\right) \left(1 + \frac{q_1^2 q_2^2}{s}\right) \cos \theta_1^* \right. \\ &\quad \left. + \left(1 - \frac{m^2}{q_2^2}\right) \left(1 + \frac{q_2^2 q_1^2}{s}\right) \cos \theta_2^* \right] \\ &\quad m^2 = \left(\frac{1}{q_1^2} + \frac{1}{q_2^2}\right) ; \quad (31) \end{aligned}$$

where the neutralino mass is kept explicitly for later discussion. This shows that the interference term behaves like  $\cos \theta_1^*$ , or  $\cos \theta_2^*$  in the massless neutralino limit. This is consistent with Fig. 5 (a).

Next, we turn to the kinematical approach to understand the Majorana effects more physically. The question is if there is a case when both amplitudes  $M_1$  and  $M_2$  of Eq. (11) are large, thus the total amplitude  $M = M_1 M_2$  is suppressed due to the relative sign from Fermi statistics. For instance, the amplitude  $M$  should be suppressed when the two neutralinos have identical spins and four-momenta. The same spin is realized by setting the  $+$  and  $-$  helicities equal in the massless neutralino limit, as previously noted. Let us determine the condition for which two neutralinos have the same four-momentum, i.e.,  $p_1 = p_2$ . It is obvious that the relative azimuthal angle is zero,  $\theta_2 - \theta_1 = 0$ . For simplicity, we consider the limit that both staus are on mass shell,  $q_1^2 = q_2^2 = m_{\tilde{\chi}_1}^2$ , where the amplitude  $M_1$  is significant. In this limit, we can find the following simple kinematical point:

$$\cos \theta_2 = \cos \theta_1 ; \quad \cos \theta_1 = ; \quad \theta_2 = \theta_1 ; \quad (32)$$

with  $= (1 - 4m_{\tilde{\chi}_1}^2/s)^{1/2}$ . At this point, not only  $q_1^2$  and  $q_2^2$  but also  $q_1^{02}$  and  $q_2^{02}$  are on  $\tilde{\chi}_1$  mass shell:

$$q_1^2 = q_2^2 = q_1^{02} = q_2^{02} = m_{\tilde{\chi}_1}^2 ; \quad (33)$$

We note that the propagator momenta squared of the crossed diagram are expressed as

$$\begin{aligned} q_{1,2}^{0,2} &= \frac{h}{8} (1 - \theta^2) (1 + \cos \theta_1 \cos \theta_2) \\ &\quad + (1 - \theta^2) \sin \theta_1 \sin \theta_2 \cos \theta_{1,2}^* \\ &\quad 2 (\cos \theta_1 + \cos \theta_2) : \quad (34) \end{aligned}$$

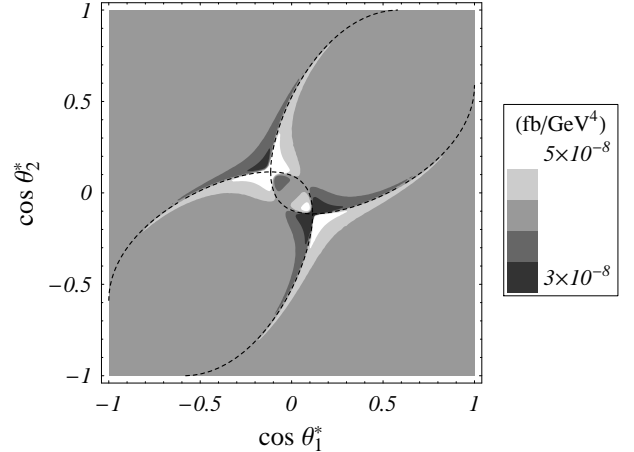


FIG. 6: Contour plot of the differential cross section, Eq. (35), for the process  $e^+ e^- \tilde{\chi}_1^+ \tilde{\chi}_1^- \tilde{\chi}_1^0 \tilde{\chi}_1^0$  at  $\sqrt{s} = 302$  GeV in the massless neutralino limit when  $q_1^2 = q_2^2 = m_{\tilde{\chi}_1}^2$  and  $\theta = 0$ , is shown in the  $\cos \theta_1^*$ - $\cos \theta_2^*$  plane, where  $\cos \theta_{1,2}^*$  are the kinematical variables defined in the  $q_{1,2}$  rest frame.  $q_1^{02} = m_{\tilde{\chi}_1}^2$  and  $q_2^{02} = m_{\tilde{\chi}_1}^2$  are also shown by dashed lines.

Fig. 6 is a contour plot of the differential cross section for the process  $e^+ e^- \tilde{\chi}_1^+ \tilde{\chi}_1^- \tilde{\chi}_1^0 \tilde{\chi}_1^0$  at  $\sqrt{s} = 302$  GeV in the massless neutralino limit when  $q_1^2 = q_2^2 = m_{\tilde{\chi}_1}^2$  and  $\theta = 0$ ,

$$\frac{d^4 p}{dq_1^2 dq_2^2 d \cos \theta_1^* d \cos \theta_2^*} ; \quad (35)$$

$$q_1^2 = q_2^2 = m_{\tilde{\chi}_1}^2 ; \quad \theta = 0$$

for the  $\theta_1 = \theta_2$  case. Using Eq. (34), we also show the  $q_1^{02} = m_{\tilde{\chi}_1}^2$  and  $q_2^{02} = m_{\tilde{\chi}_1}^2$  trajectories by dashed lines. The interference effect can be seen along these lines, especially around the intersection points, where both  $q_1^{02}$  and  $q_2^{02}$  approach  $m_{\tilde{\chi}_1}^2$  and the effect is largest. This arises from the double Breit-Wigner factor  $D(q_1^{02})D(q_2^{02})$  of the crossed amplitude  $M_2$ . Note also that the sign of the interference term changes over the  $q_1^{02} = m_{\tilde{\chi}_1}^2$  or  $q_2^{02} = m_{\tilde{\chi}_1}^2$  trajectory because of the Breit-Wigner resonant factor. Around one of the intersections (black region), which corresponds to the kinematical point of Eq. (32) with

$\theta = 0.115$ , the cross section is strongly suppressed because the two neutralinos have the same momentum. On the other hand, it is enhanced around another intersection (white region), i.e.,  $(\cos \theta_1^*; \cos \theta_2^*) = (0; 0)$ . That is because the four-momenta of the  $+$  and  $-$  leptons become identical at this point, and the two interfering amplitudes are constructive. Here one can also see negative interference for  $\cos \theta_1^* > 0$  ( $\cos \theta_2^* < 0$ ) and constructive interference for  $\cos \theta_1^* < 0$  ( $\cos \theta_2^* > 0$ ).

Let us now try to explain the consistency among the three distributions  $\cos \theta_1^*$ ,  $E$ , and  $M(\sim)$  in Fig. 5. In the phase space limit of  $M(\sim) = 2m_{\tilde{\chi}_1}^2 = 0$ , the four-momenta of the two neutralinos are identical ( $p_1 =$

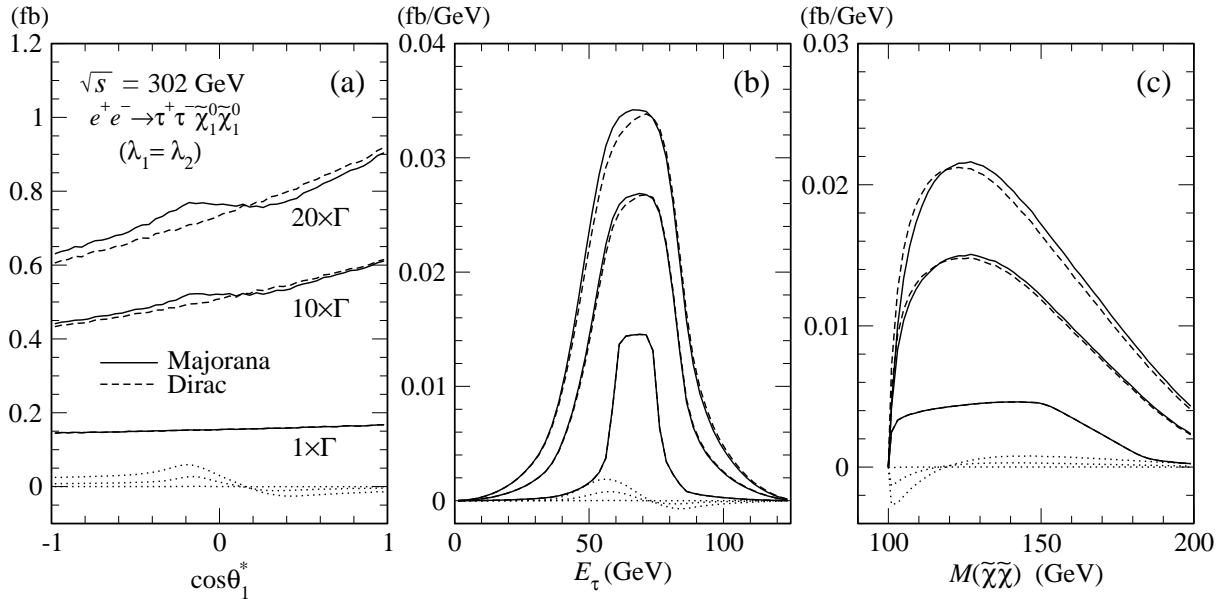


FIG. 7: Distributions of (a)  $\cos \theta_1^*$ , (b)  $E_\tau$ , and (c)  $M(\tilde{\chi}\tilde{\chi})$  for the process  $e^+ e^- \rightarrow \tau^+ \tau^- \tilde{\chi}_1^0 \tilde{\chi}_1^0$  for the  $\lambda_1 = \lambda_2$  case at  $\sqrt{s} = 302$  GeV for  $1, 10, 20 \times \Gamma$ . Solid and dashed lines show the Majorana and Dirac neutralino cases, respectively. Also shown is the behavior of the interference term by dotted lines.

$p_2$ ). As discussed above, therefore, negative interference should be expected near this limit due to Fermi statistics. Furthermore, when  $q_1^0 = q_2^0 = m_{\tilde{\chi}}^2$  in this limit, it is obvious that the amplitude is suppressed in the region  $\cos \theta_1 > 0$  and  $\cos \theta_2 < 0$ . In addition, due to boost effects, this kinematical region corresponds to large  $E_\tau$ .

So far all our distributions have been given for massless neutralinos. Let us now show results for finite neutralino masses.

Fig. 7 is the same as Fig. 5, except we include the single-resonance contributions to the final state and a finite neutralino mass,  $m_{\tilde{\chi}}^0 = 50$  GeV. Since the single-resonance contributions are not so small just above the stau pair threshold (see Fig. 4), the distributions are affected significantly. As for the  $M(\tilde{\chi}\tilde{\chi})$  distribution, the lowest value of the invariant mass is  $2m_{\tilde{\chi}}^0 = 100$  GeV in this case. We find that the interference pattern is basically the same as in Fig. 5, where we consider only the  $\tilde{\chi}_1$  pair production process in the  $m_{\tilde{\chi}}^0 = 0$  limit.

However, one can also see a difference in the behavior of the interference between Fig. 7 and Fig. 5. The region of constructive interference becomes larger than that in Fig. 5. The reason is given by Eq. (31): the third term proportional to the neutralino mass squared is additive with the first term,  $\cos \theta_1$ , when we consider a finite neutralino mass.

We can also repeat the kinematical analysis for the Majorana case, taking into account a finite neutralino mass. Eq. (32) is slightly modified by the boost effect as

$$\cos \theta_2 = \cos \theta_1; \quad \cos \theta_1 = \frac{1 + m_{\tilde{\chi}}^2 - m_{\tilde{\chi}}^2}{1 - m_{\tilde{\chi}}^2 - m_{\tilde{\chi}}^2} > 0; \quad (36)$$

where the two neutralinos have the same momentum. On the other hand, the condition that the momenta of  $\tau^+$  and  $\tau^-$  are the same does not change, namely  $(\cos \theta_1; \cos \theta_2) = (0; 0)$ . This supports the tendency of the interference pattern to increase with finite neutralino mass in Fig. 7.

Fig. 8 is the same as Fig. 7, but for the  $\lambda_1 \neq \lambda_2$  case. As we discussed and explicitly showed in Eq. (26) at the end of Sec. III, one can see the Majorana interference effect even for the  $\lambda_1 \neq \lambda_2$  case. The distributions for the  $\lambda_1 = \lambda_2$  case are much more useful than those of the  $\lambda_1 \neq \lambda_2$  case because in (a) there is a significant shape change which includes two injection points, whereas the distribution is monotonic in the latter case; and because in (b,c) the distributions for  $\lambda_1 = \lambda_2$  involve a peak shift, not just a magnitude change as for  $\lambda_1 \neq \lambda_2$ .

A final question we may ask is, what would be the observability of the Majorana interference effect? We answer this by calculating the integrated luminosity required at a future linear collider to observe a 3-sigma effect, using the case MSSM described above and collisions at  $\sqrt{s} = 302$  GeV. The simplest observable is the  $\cos \theta_1$  distribution of Fig. 5 (a), which has a small forward-backward asymmetry  $A$ . We furthermore make the estimate using the non-physical enhanced effect case of  $10 \times \Gamma$ . The formula for the statistical uncertainty on an asymmetry measurement is,

$$4A = \frac{P}{N_F (2N_B - N^2)^2 + N_B (2N_F - N^2)^2}; \quad (37)$$

where  $N_F$  ( $N_B$ ) is the number of events with  $\cos \theta_1 > 0$  ( $\cos \theta_1 < 0$ ) and  $N = N_F + N_B$  is the total number of events. Since the asymmetry is small, 0.02 in this case, we may use the approximation  $N_F = N_B = N/2$ .

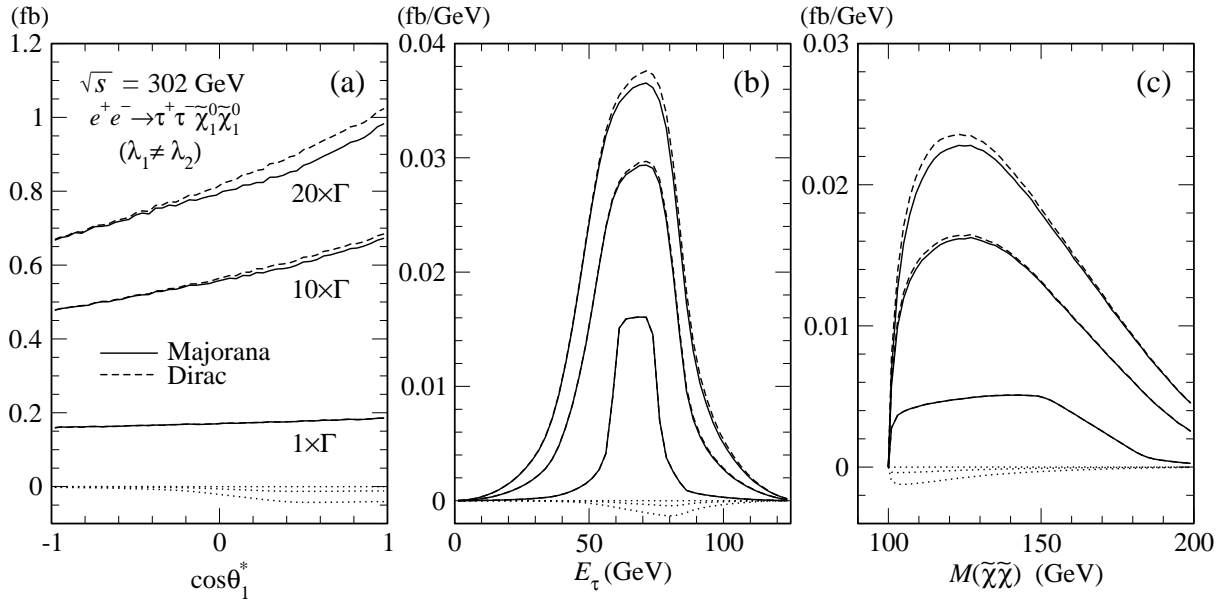


FIG. 8: The same as Fig. 7, but for the  $1-2$  case.

Substituting and rearranging, we arrive at a formula for the required luminosity to observe a 3% effect:

$$L_{\text{min}} = (3A)^2 = L_{\text{total}} : \quad (38)$$

Plugging in  $A = 0.02$  and  $L_{\text{total}} = 12 \text{ fb}$ , we arrive at an estimate of  $18,750 \text{ fb}^{-1}$ . One is swift to conclude that even in an enhanced-effect scenario due to abnormally large finite stau width, a future linear collider unfortunately cannot observe this effect.

## V I. SUMMARY AND DISCUSSIONS

We studied the quantum mechanical correlation between two identical neutralinos, which exists only if they are Majorana particles, for the process  $e^+ e^- \rightarrow \tilde{\chi}_1^0 \tilde{\chi}_1^0$ . We also considered the single-resonance contributions to the final state.

We found that the correlation between two neutralinos appears near the pair production threshold in the presence of a finite stau width and mixing of the staus and/or neutralinos. We discussed the finite width effect in detail, and found that the correlation effect tends to be proportional to the decay width. Distributions in several kinematical variables, such as  $\cos\theta_1^*$ ,  $E_\tau$  and  $M(\tilde{\chi}\tilde{\chi})$  as defined in Sec. V, show the interference effect, although the effect largely disappears after integrating over these distributions. Because the correlation effects are significant only in a specific kinematical configuration, they can be observed only in models where the neutralino momenta can be kinematically reconstructed, such as in models with R-parity violation. Unfortunately the interference pattern does not persist in the angular distribution of the final-state taus in the lab frame, disallowing these

observables to be determined in an R-parity-conserving MSSM scenario.

Our brief estimate of the potential observability of the Majorana interference effect (assuming an R-parity-violating scenario) using the asymmetry of the stau decay angular distribution in its rest frame is unfortunately not optimistic. It appears that an unrealistic amount of integrated luminosity at a future  $e^+ e^-$  collider operating at stau pair threshold would be required. Thus this particular interference effect for stau NLSP pairs remains a pedagogical observation, but a very interesting one nonetheless.

Before closing our discussions, we point out that a significant interference effect is also expected in  $e_L e_R$  and  $\tilde{\chi}_L \tilde{\chi}_R$  pair production processes. The quantitative study will be reported elsewhere.

## Acknowledgments

K.M. would like to thank M. Aoki, E. Senaha, H. Shimizu, and H. Yokoya for discussions and encouragement. The work of K.H. is supported in part by the Grant-in-Aid for Scientific Research, Ministry of Education, Culture, Science and Technology, Japan (No 17540281).

---

[1] S. Dawson, E. Eichten and C. Quigg, *Phys. Rev. D* 31, 1581 (1985).

[2] J.R. Ellis and G.G. Ross, *Phys. Lett. B* 117, 397 (1982).

[3] P.J. Fox, A.E. Nelson and N.W. einer, *JHEP* 0208, 035 (2002) [[arXiv:hep-ph/0206096](https://arxiv.org/abs/hep-ph/0206096)].

[4] S. T. Petcov, *Phys. Lett. B* 139, 421 (1984); S. M. Bilenky, N. P. Nedelcheva and E. K. Khrustova, *Phys. Lett. B* 161, 397 (1985); G. M. Oortgat-Pick and H. Fraas, *Eur. Phys. J. C* 25, 189 (2002).

[5] J.A. Aguilar-Saavedra and A.M. Teixeira, *Nucl. Phys. B* 675, 70 (2003).

[6] S. Y. Choi and Y. G. Kim, *Phys. Rev. D* 69, 015011 (2004).

[7] M. M. Nojiri, *Phys. Rev. D* 51, 6281 (1995).

[8] M. M. Nojiri, K. Fujii and T. T. Suzuki, *Phys. Rev. D* 54, 6756 (1996).

[9] A. Denner, H. Eck, O. Hahn and J. Kublbeck, *Nucl. Phys. B* 387, 467 (1992).

[10] H. Murayama, I. Watanabe, and K. Hagiwara, *KEK Report* 91-11 (1992).

[11] S. Kawabata, *Comput. Phys. Commun.* 88, 309 (1995).